Using the space-borne NASA Scatterometer (NSCAT) to determine the frozen and thawed seasons of a boreal landscape

S. Frolking[1]*, K.C. McDonald[2], J.S. Kimball[3], J.B. Way[2], R. Zimmermann[4], S.W. Running[3]

[1]Institute for the Study of Earth, Oceans, and Space and Dept. of Earth Sciences, U. New Hampshire, Durham NH 03824

[2]Jet Propulsion Laboratory, California Institute of Technology , Pasadena CA 91109

[3]School of Forestry, U. Montana, Missoula MT 59812

[4]Bitöek, U. Bayreuth, Bayreuth, D-95540 GERMANY

*Corresponding Author:
Steve Frolking
Inst. for the Study of Earth, Oceans, and Space
Morse Hall
39 College Rd.
Durham NH 03824
ph: 603-862-0244
fax: 603-862-0188
e-mail: steve.frolking@unh.edu

Manuscript for submission to JGR-Atmospheres - second BOREAS compilation.

Submitted on: 24 July 1998

Revised: 22 Oct 1998

KEYWORDS: NSCAT, remote sensing, radar, BOREAS, freeze, thaw, growing season

ABSTRACT: We hypothesize that the strong sensitivity of radar backscatter to surface dielectric properties, and hence to the phase (solid or liquid) of any water near the surface, should make space-borne radar observations a powerful tool for large-scale spatial monitoring of the freeze/thaw state of the land surface, and thus ecosystem growing season length. We analyzed the NASA Scatterometer (NSCAT) backscatter from 9/96 through 6/97, along with temperature and snow depth observations, and ecosystem modeling, for three BOREAS sites in central Canada. Because of its short wavelength (2.14 cm) NSCAT was more sensitive to canopy and surface water than to water deeper in the soil. NSCAT had 25 km spatial resolution and approximately twice-daily temporal coverage at the BOREAS latitude. At the northern site the NSCAT signal showed strong seasonality, with backscatter around -8 dB in winter and -12 dB in early summer and fall. The NSCAT signal for the southern sites had less seasonality. At all 3 sites there was a strong decrease in backscatter during spring thaw (4-6 dB). At the southern deciduous site, NSCAT backscatter rose from -11 to -9.2 dB during spring leafout. All sites showed 1-2 dB backscatter shifts corresponding to changes in landscape water state coincident with brief mid-winter thaws, snowfall, and extreme cold ($T_{max} < -25°C$). Existing radar freeze/thaw detection algorithms gave reasonable results for the northern site, but were not successful at the 2 southern sites. We developed a change detection algorithm based on first differences of 5-day smoothed NSCAT backscatter measurements. This algorithm had some success in identifying the arrival of freezing conditions in the autumn and the beginning of thaw in the spring. Changes in surface freeze/thaw state generally coincided with the arrival and departure of the seasonal snow cover and with simulated shifts in the directions of net carbon exchange at each of the study sites.

1. INTRODUCTION

The transition of the land surface from a frozen to thawed state represents the closest analog to a biospheric on/off switch existing in nature. This transition strongly affects ecological trace gas dynamics, surface meteorological conditions, and landscape hydrologic activity. The timing of ecosystem freeze-up and thaw, and thus the duration of both the growing and dormant seasons for plants, can be expected to change with climatic change. A climatic warming will likely lead generally to earlier thaws, later freeze-ups and a longer growing season. There is also a large range in interannual variability (up to 6 weeks or more) in the timing of freeze and thaw at a given location [e.g., *Frolking et al.*, 1996].

The timing of spring thaw and the duration of the growing season are strongly linked to the carbon balance of boreal and arctic systems. In both empirical [*Goulden et al.*, 1997] and process [*Frolking et al.*, 1996; *Frolking* 1997] boreal ecosystem modeling studies, earlier spring thaws led to significant increases in net carbon uptake. Eddy covariance carbon flux measurements have shown enhanced carbon uptake associated with earlier spring thaws in both temperate forest [*Goulden et al.*, 1996] and boreal forest stands. At the BOREAS southern aspen site, the transition of the ecosystem from a carbon source (~25 kg C/ha/d loss) to its maximum rate of carbon uptake (~75 kg C/ha/d uptake) occurs over a 10 day period in the spring of both 1994 and 1996 (data were not collected in 1995); an earlier spring at this site in 1994 yielded an additional ~0.67 Mg C net uptake compared with spring 1996 [*Black et al.*, 1996 & unpublished data]. For this deciduous stand, the ecosystem transition from a carbon source to a carbon sink lagged soil thaw by about 5 weeks in both 1994 and 1996. At the BOREAS northern and southern black spruce sites, the ecosystem's transition from carbon source to sink is coincident with snowmelt and soil thaw [*Goulden et al.*, 1997; *Jarvis et al.*, 1997 & unpublished data]. Increased vegetation activity at high latitudes has been inferred from both the atmospheric CO_2 concentration record [*Keeling et al.*, 1996] and the Advanced Very High Resolution Radiometer (AVHRR) Normalized Difference Vegetation Index (NDVI) record [*Myneni et al.*, 1997]. The 1981-1990 surface temperature record shows a significant warming trend (~2-4°C) for the late winter/early spring for northern latitudes (>45°N) [*Myneni et al.*, 1997]. Soil temperature simulations from

1976-1996 for boreal forest stands, using the model of *Frolking et al.* [1996], show 6-7 week ranges in the timing of soil thaw at 3 cm.

There have been a number of applications of microwave sensors to detect freeze/thaw transitions in terrestrial ecosystems. The microwave backscatter signature of a landscape is controlled by the landscape's structure and dielectric properties [*Elachi*, 1987]. The interaction of an electric field with a dielectric material has its origin in the response of charged particles to the applied field. The displacement of these particles from their equilibrium positions gives rise to induced dipoles that respond to the applied field. In addition, polar materials contain permanent dipoles caused by the asymmetric charge distribution within the molecules themselves [*Kraszewski*, 1996]. Consisting of highly polar molecules, liquid water exhibits a dielectric constant that dominates the microwave dielectric response of natural landscapes. As water freezes, the molecules become bound in a crystalline lattice, and the dielectric constant decreases substantially. For vegetated landscapes that undergo freeze/thaw transitions, this drop in dielectric constant results in a large decrease in L-band (15 – 30 cm wavelength) and C-band (3.75 – 7.5 cm wavelength) backscatter [*Way et al.*, 1994; *Way et al.*, 1997]. In addition, microwave sensors are active systems providing their own illumination source and receiving that which is scattered from the surface thus providing observations day and night, independent of seasonal sun angles. Also, microwave sensors operate at relatively long wavelengths thereby 'seeing through' clouds, aerosols and smoke, which obscure the land surface at optical wavelengths. Continuous access to surface state is available 365 days a year and in any weather; actual coverage is therefore defined by a mission's orbit design.

Studies using truck-mounted scatterometers have shown that radar backscatter from frozen ground and frozen vegetation is significantly different than the radar backscatter from thawed ground and vegetation [*Ulaby et al.*, 1982]. *Wegmuller* [1990] measured a 3-4 dB drop in radar backscatter from bare soils during day-night freeze/thaw cycles. Backscatter change resulting from freezing and thawing was first observed in radar image data in a series of aircraft radar data sets that were acquired over the Bonanza Creek Experimental Forest, a Long Term Ecological Research (LTER) site near Fairbanks, Alaska in March 1988 [*Way et al.*, 1994].

During the time period over which the imaging radar data were collected, temperatures ranged from unseasonably warm (up to 9°C) to well below freezing (-8 to -15°C), and the free water in the trees changed from a liquid to solid phase. These imaging radar data showed a 4 to 6 dB decrease in the radar backscatter of the forest stands with freezing.

With the launch of ERS-1 in 1991, an intensive study of the fall freeze transition was carried out in Alaska [*Rignot et al.*, 1994]. ERS-1 C-band images were acquired of the Tanana River floodplain forests. Canopy and soil temperatures and meteorological data were collected in three representative stands; black spruce, white spruce and balsam poplar. The data show that a 3 dB drop in backscatter occurs during the trees' transition from a thawed to a frozen state. The results of this work were applied on a landscape scale by *Rignot & Way* [1994]. Transects of 200 m resolution ERS-1 radar data which crossed Alaska from north to south were collected from August through November 1991. Freezing as observed in the image transects was consistent with meteorological data collected along the transects; the data show that, as is expected, freezing occurs first in the high latitude and high altitude regions. In the autumn, backscatter decreased to reflect frozen conditions and remained stable during early snowpack accumulation [*Rignot & Way,* 1994].

ERS-1 imaging radar data from the 1994 BOREAS experiment showed a two-stage shift in backscatter, the first coincident with observed soil thaw in March and the second with canopy thaw in May [*Way et al.*, 1997]. Tree bole and soil temperature data at the southern black spruce site showed a transition from completely frozen soil to the onset of soil thaw on yearday 60. The water in the tree stems thawed on yearday 100 and remained at or above 0°C after this date. The ERS-1 data show a significant rise in backscatter between yearday 60 and 63, and again between yearday 78 and 102 [*Way et al.*, 1997]. These shifts in ERS-1 backscatter were concurrent with ecosystem model simulations of shifts in net ecosystem exchange of carbon dioxide with the atmosphere [*Way et al.*, 1997; *Kimball et al.*, 1997; *Frolking et al.*, 1996].

Boehnke & Wismann [1997] used the ERS-1 scatterometer to detect soil thaw in Siberia, resampling backscatter data from 1 March 1993 to 1 July 1993 to a 50x50 km grid and computing a 3-day average backscatter. They proposed as an ERS scatterometer freeze/thaw detection algorithm that the landscape thaws (freezes) when two consecutive backscatter values exceed (drop below) the average of all July (thawed) and all February (frozen) backscatter values [*Boehnke & Wismann,* 1997]. By requiring two consecutive signals above or below the threshold value, the algorithm will not be triggered by brief freeze/thaw events or spikes in the data. It also will not detect or interpret signals like the large drop in backscatter (below the frozen winter values) that occurred at their northern location.

In this paper we explore the usefulness of radar backscatter data from NSCAT for detecting boreal ecosystem freeze/thaw transitions at sites in the BOREAS study area in central Canada. NSCAT had a broader swath width than the ERS-1 scatterometer, providing coarser spatial resolution (25 km) and higher temporal (twice-daily) resolution coverage. NSCAT had a higher frequency (shorter wavelength) than the ERS-1 SAR and scatterometer, providing a different sensor configuration, and thus somewhat different scattering physics.

2. SITES AND DATA

2.1. Field Sites

We chose three field sites from the BOREAS program for our study: the Northern Old Black Spruce (NOBS) site near Thompson, Manitoba (55.9°N, 98.5°W), the Southern Old Black Spruce (SOBS) site near Nipawin, Saskatchewan (54.0°N, 105.1°W), and the Southern Old Aspen (SOA) site in Prince Albert National Park, Saskatchewan (53.6°N, 106.2°W). All three of these sites had eddy covariance flux towers operating during the BOREAS program in 1994 and 1996, and the towers at NOBS and SOA continue to operate. Since the operation period for NSCAT was Sept. 1996 through June 1997, and thus generally outside the BOREAS field campaign periods and beyond the BOREAS meteorological network operational period [*Sellers et al.,* 1997], we have taken weather data from two stations operated by the Canadian AES [Thompson, Manitoba and Nipawin, Saskatchewan) that have reported 1996 and 1997 data; these data were

obtained from the National Climate Data Center Summary of the Day, First Order TD-3210 database (http://www4.ncdc.noaa.gov/ol/documentlibrary/datasets.html#TD3210). These stations reported daily maximum and minimum temperatures, daily total precipitation, and daily snow depth on the ground. The Nipawin station was located approximately 78 km south-east of the SOBS site while the Thompson station was located approximately 45 km south-east of the NOBS site.

2.2. NASA Scatterometer (NSCAT)

NSCAT flew on board the Advanced Earth Observing Satellite (ADEOS), a mission of the National Space Development Agency of Japan (NASDA). The platform was launched August 16, 1996 into a near-polar Sun-synchronous orbit and operated through June 30, 1997 when the mission terminated because of power failure. The NSCAT instrument package consisted of a specialized microwave radar designed for measuring wind vectors over the global ocean [*Naderi et al.*, 1991]. The scatterometer operated at a frequency of 13.995 GHz (K_u band, corresponding to a 2.14 cm wavelength) and utilized an array of six antennas, providing both right- and left-looking 600 km-wide radar swaths, separated by a gap of approximately 330 km. Incidence angle varied across each swath from approximately 15° off-nadir in the near range to 60° in the far range. This configuration allowed coverage of 90% of Earth's surface every two days. The overall backscatter measurement stability was about 0.3 dB [*Tsai et al.*, 1998].

Although the primary focus of the NSCAT mission was on monitoring ocean wind vectors, the high temporal fidelity of the data set provides opportunity for research into observation of landscape temporal dynamics. In our analysis, we utilize the NSCAT High-Resolution Merged Geophysical Data Product [*Dunbar*, 1996] to examine 25 km resolution cells over the BOREAS sites. NSCAT data were available for the BOREAS sites for 286 days, from 15 Sept 1996 through 28 June 1997. NSCAT overflights at the BOREAS sites occurred in the early morning (0515-0730) and late afternoon (1530-1750) at these BOREAS sites. AM and PM overflights were each recorded on ~70% of the days, and ~5% of the days at the northern site and ~14% of the days at the southern sites had no NSCAT observations. Each resolution grid cell was normalized to 40° incident angle through application of a linear function that describes the angular

dependence of backscatter over the landscape [*Kennett & Li*, 1989]. In this analysis, we used measurements acquired with NSCAT's aft vertically polarized antenna. The data were then aggregated over the 50 km regions centered over the tower locations by averaging all backscatter pixels whose centers were within 25 km of the tower latitude/longitude. On days when there were two data values for a site (always separated by 100 minutes, and so on consecutive orbits), we chose the earlier overpass as it was more likely to correspond to the time of the diurnal minimum or maximum temperature, and thus to potential freeze or thaw signals.

2.3. Landcover Analysis

Although there are only a few tree species in the boreal zone [e.g., *Elliott-Fisk*, 1988] and the central Canadian topography is quite flat, the boreal landscape is very heterogeneous. This heterogeneity is due in part to patchy disturbances (e.g., fire), discontinuous permafrost in the north, low topographic gradients and excess moisture generating local wetlands, and beaver activity [e.g., *Larsen*, 1980]. A great deal of effort in the BOREAS program has been and is being devoted to characterizing the landcover at various spatial resolutions, and to understanding the implications of this varied landscape on biosphere-atmosphere interactions [e.g., *Steyaert et al.*, 1997, *Hall et al.*, 1997; *Ranson et al.*, 1997]. Landcover classifications have been developed using optical remote sensing at both ~1 km resolution (AVHRR; [*Steyaert et al.*, 1997]) and ~30 m resolution (Landsat TM; [*Steyaert et al.*, 1997]). We summarize these results as percentage cover for the 50x50 km NSCAT windows centered on the BOREAS tower sites in Table 1. In general, landcover at SOA and to the southwest of this is predominantly deciduous and mixed conifer/deciduous (i.e., at least 20-80% of each class) forest dominated by aspen *(Populus tremuloides),* jack pine *(Pinus banksiana)* and black spruce *(Picea mariana)* stands. The SOBS region (about 80 km to the east of SOA) is much more dominated by the wet conifer class (i.e.,. muskeg or black spruce peatlands). Agricultural development, consisting of both row crops and pasture, is also present in the southern portions of the SOA and SOBS windows but is absent within the NOBS study region; this landcover is in the 'disturbed' class in the AVHRR data in Table 1. These areas are represented in the AVHRR landcover classification but are not fully represented in the TM classification due to incomplete TM coverage within

the SOA window (see Table 1). Many small scale landscape features (e.g., fens) cannot be resolved at 1 km and thus are probably under-represented in the AVHRR analysis, and perhaps also in the TM analysis. To the south and south-east of the NOBS tower, and within the NSCAT pixel and landcover analysis (Table 1), are large fire scars. These areas are regrowing and were identified as regenerating conifer and regenerating deciduous forest from the TM classification map. Similar, though less extensive fire scarred areas within the SOBS window (part of the 1977 Fish Lake burn) are dominated by small (< 5 cm diameter at breast height) jack pine, black spruce and aspen regrowth [*Hall et al.*, 1997, *Saatchi & Rignot*, 1997].

2.4. Soil Temperature Simulations

Soil temperatures were not reported in the BOREAS database for the spring of 1997, so we simulated soil temperatures using the model of *Frolking et al.* [1996]. Simulations were run for each of the BOREAS tower sites, driven by daily meteorological observations at Thompson and Nipawin. For the NOBS site, two ground cover classes were simulated, with black spruce underlain by either feathermoss or sphagnum moss. Time of thaw at 5 cm was in good agreement with observations at NOBS [*Goulden et al.*, 1997] in 1995 and 1996 for both groundcover types (Fig. 1). For all three sites, the surface organic horizons that were >5 cm thick, so 5 cm soil depth was above the mineral soil.

3. ANALYSIS AND RESULTS

3.1. AM and PM Differences

At each location AM and PM NSCAT backscatter signals had similar seasonalities, though the PM overflights often had greater variability from one day to the next (Fig. 2). AM overflights occurred in the early morning and should be roughly coincident with the diurnal minimum temperature and thus the maximum degree of frost, while PM overflights were in late afternoon and should be roughly coincident with the diurnal maximum temperature and thus the minimum degree of frost. PM backscatter values were generally lower than AM values for the two coniferous sites during the spring and early summer of 1997, and were more dynamic than the AM overflights during the period of snowmelt and thaw.

3.2. NSCAT Backscatter and Environmental Variables

To generate a smoothed AM or PM signal, we calculated for each day the average of that day's and the previous four days' backscatter values (in a few cases with missing values these averages used only 1 or 2 data points). This smoothing was done for each site on AM and PM data separately, and also on the combined AM and PM data sets.

Major fluctuations in the NSCAT backscatter (σ^0) time series for the NOBS site showed a strong correlation with environmental variables (Fig. 3a). The first significant rise in σ^0 (2 dB) occurred with the arrival of the first snow. A second, stronger rise in σ^0 (3 dB) occurred after a melt with the re-establishment of snow cover and a drop in temperature around Nov. 1, 1996. There was then a brief drop in σ^0 with a warmer period and perhaps some melting of the snow. The third rise in σ^0 (2.5 dB) occurred several days after the third heavy snowfall when the air temperatures got quite cold ($T_{max} < -30°C$). σ^0 dropped 2 dB in early February 1997 when T_{max} rose above 0°C, then rose again when the weather cooled. Several days with $T_{max} > 0°C$ in late March 1997 caused σ^0 to drop below -10 dB, then a week of cold weather sent σ^0 back up to -7 dB. σ^0 plunged to -13 dB as the snowpack melted, and σ^0 rebounded to around -11 dB when the snowpack was gone. Note that the soil did not thaw at 5 cm depth until several weeks after the backscatter had returned to its thawed range (Fig. 3a). There was a strong seasonality to σ^0 at the NOBS site, which correlated with air temperature ($r^2 \sim 0.6$) and snow depth ($r^2 \sim 0.4$). NSCAT backscatter values at the two southern sites (Fig. 3b,c) also showed fluctuations coincident with changes in snowpack and large temperature fluctuations; the deciduous site (SOA) exhibited the least amount of variation with seasonal transitions although the dynamic range in the backscatter temporal response to the 1997 springtime thaw was similar for all three sites.

3.3. First Differences of the NSCAT Signal

We calculated the first difference of the smoothed NSCAT AM and PM signals for each site (first difference equals σ^0 of day *i* minus σ^0 of day *i-1*). These first differences were normally distributed about a near-zero mean (Table 2), and we calculated the standard deviation of the first differences. To select those periods

when the backscatter was most dynamic, we identified those first differences which were more than 2 standard deviations from the mean (Fig. 4). The numbers of days with first differences outside 2 standard deviations ranged from 11 at the SOA AM overflights to 16 for all PM overflights (Table 2).

4. DISCUSSION AND CONCLUSIONS

4.1. Detecting Freezing and Thawing

One algorithm developed for detecting freezing and thawing from ERS-1 SAR microwave backscatter relied on a 3 dB change in backscatter from the thawed values observed in mid-summer (*Rignot & Way*, 1994]. Since there are no NSCAT data from mid-summer (July) due to platform failure, we used the June mean σ^0 for morning and evening overflights at each sight to represent the signal for the thawed state (Table 2). We then computed the difference from this mean for the five-day smoothed σ^0 for each overflight time. Using a 3 dB threshold does not account for variation in backscatter sensitivity to freeze/thaw transitions driven by gross landscape features (e.g. topography, vegetation cover, etc.). This technique would predict only intermittent freezing at the northern site and no real freezing at the southern sites, despite air temperatures as low as -40°C.

Boehnke & Wismann [1997] proposed the mean of summer and winter ERS-1 scatterometer backscatter as a freeze/thaw threshold. They observed a 3-4 dB increase in backscatter from test sites in Siberia during spring thaw, which they attribute to snowmelt, but without any ground observations. We observe different temporal trends in the NSCAT data sets, with spring thaw resulting in decreasing backscatter. The ERS-1 scatterometer has a frequency of 5.3 GHz (wavelength = 5.7 cm), 2.66 times longer than NSCAT. The difference in NSCAT and ERS-1 temporal responses to changes in landscape freeze/thaw state arises in part from variations in relative contribution to the composite backscatter of surface and volume scattering effects. *Boehnke & Wismann* [1997] observed an increase in the volume scattering component of the composite ERS backscatter from sparse vegetation cover after thaw. Examination of NSCAT winter and spring data indicate no such variation over forested areas. In general, the energy from the higher frequency scatterometer penetrates less into the vegetation medium, yielding less volume scattering. Applying the

algorithm of *Boehnke & Wismann* [1997] to the NSCAT data, using the June mean to represent the thawed state and the February mean for the frozen state (Table 2), the NOBS site would freeze on Nov. 1, thaw briefly and re-freeze a week later, thaw briefly on March 27, and thaw for the summer on April 18 (Fig. 5a). The SOBS site would freeze briefly on Nov. 22, freeze again on Dec. 19, thaw briefly on Feb. 6; thaw on March 22; freeze briefly on April 6, and thaw for the summer on April 18 (Fig. 5b). For the SOA site AM and PM overflights the June (thawed) mean σ^0 values were higher than the February (frozen) mean σ^0 values (Table 2). This freeze/thaw algorithm would have the site freezing and thawing throughout the winter (Fig. 5c), and then freezing up on June 11 until the end of the instrument record (June 30). This final rise in backscatter (interpreted by this algorithm as a freeze-up) was more likely due to a rise in deciduous vegetation leaf area than to freezing (see Section 4.3 below).

Evaluating 'anomalous' first differences of the smoothed σ^0 signal (more than 2 standard deviations from the mean; see Fig. 3) may also be able to identify changes in the landscape freeze/thaw state. Most days with anomalous first differences were coincident with either fresh snowfall or snowmelt (Tables 3 and 4). The late September anomalies at the SOBS site may be due to missing data (25-27 Sept.) and thus less smoothing (though a similar data gap at this site 15 days later did not generate first difference anomalies) or to changes in leaf water content as the canopy senesced. At the time of snowmelt, all sites show a number of large, consecutive first difference anomalies, corresponding with both warmer air temperatures (T_{air} > 0°C), decreasing snow depths, a wetter snowpack, and new snowfall. Not every snow storm generated a first difference anomaly signal. This may be due to spatial heterogeneity in precipitation, i.e., differences in precipitation between a point measurement from a single station and precipitation characteristics within the 50 x 50 km NSCAT window. Another reason might be that snowpack characteristics do not necessarily change with each new storm, and do not change only with a snow storm. However, without better instrumentation (e.g., more stations, snow density and crystal size measurements) this cannot be documented. These anomalies in the first difference of the NSCAT smoothed backscatter signal might be useful as a detection algorithm for changes in snowpack properties and canopy freeze/thaw state, but not to soil freeze/thaw.

The strongest signal in the 9 month NSCAT backscatter record was the ~3-6 dB decrease that occurred with snowpack ripening and melting in the spring. Soil thaw generally lags snowmelt by days (depths of a few cm) to weeks (depths of tens of cm). Tree bole temperatures measured in 1994 at the SOBS site [*Way et al.*, 1997] were very similar to observed air temperatures, so any melting of the snowpack would be coincident with a thawing of the tree canopy, which would also contribute to a change in the NSCAT signal. In the north this was a single event which began on 11 April 1997; in the south the melt began on 15 March 1997, was interrupted by a period of re-freezing beginning on 2 April, 1997, and a final melting beginning on 11 April, 1997. This suggests that NSCAT detected north-south variations spring thaw, a key ecosystem growing season signal.

4.2. Snowpack Dynamics and Comparison to ERS Scatterometer

NSCAT σ^0 values appear to be much more variable throughout the frozen season than ERS-1 σ^0 values [*Boehnke & Wismann,* 1997]. Since the vegetation canopy structure probably changed very little over the 9 months of NSCAT operation (except for deciduous vegetation leaf development discussed below), the variability in the σ^0 signal is probably due to changes in snow cover (including snow caught in the tree canopy), changes in snow properties (particularly near the snow surface), and changes in relative amounts of liquid and frozen water of the vegetation canopies. NSCAT σ^0 values are not likely to be strongly influenced by the state of the soil, except for areas with scant or no vegetation (e.g., recent disturbance sites). The longer wavelength ERS scatterometer will penetrate deeper into the scattering volume (canopy, snowpack, and soil) and be more influenced by volume scattering than surface scattering, which may account for the smoother winter signal reported by [*Boehnke & Wismann*, 1997].

Bulk snowpack densities were measured in the BOREAS study areas in the winters of 1993-4, 1994-5, and 1995-6; bulk density rose slowly through the winter from ~0.1 g/cm^3 to ~0.18 g/cm^3 and then at the onset of melting (around April 1 each year) rose rapidly to ~0.3 g/cm^3 [B. Goodison et al., unpublished BOREAS data]. The only snowpack data available to this study for the winter of 1996-7 were the daily observed snow

depths at the weather stations in Thompson and Nipawin. While snow depth data give crude information (arrival of snow and timing of major snow melts in particular) they do not provide any details on the changing characteristics of the snow cover which can influence the microwave backscatter at the NSCAT frequency. Dry snow will have a very small absorption of microwaves, while liquid water in wet snow is strongly absorbing [*Kunzi et al.*, 1982]. Inhomogeneities in the snow structure can have dimensions comparable to the NSCAT wavelength (~2 cm) and thus can cause significant volume scattering [*Shi et al.*, 1993; *Kunzi et al.*, 1982]. However, snowpack structure can vary significantly throughout a winter [e.g., *Colbeck*, 1982], and these changes can influence how microwaves interact with the snowpack [*Wankiewicz*, 1993]. In addition, the characteristics of the snowpack can change dramatically across the landscape; digging detailed snow pits in a transect across northern Alaska, *Hall et al.*, [1991] found seven different classes of snow (new snow, melt-freeze layer, small rounded snow grains, large rounded snow grains, wind crust, depth hoar crystals, and partially decomposed precipitation particles) within 10 cm of the snowpack surface. NSCAT's short wavelength will make it sensitive to this level of detail in the snowpack properties. In addition, the NSCAT signal will be very sensitive to the amount and characteristics of snow held by the vegetation canopy.

During the snowmelt period, the boreal landscape will transform from snow-covered first to a mosaic of wet (melting) snow and snow-free patches with a very wet surface layer (often organic material) and frozen soil deeper down, and finally to a snow-free, generally wet surface with thawing soils at depth. During this period, the vegetation will also thaw, yielding associated increases in vegetation dielectric constant, simultaneous with changes in the underlying snow and soil. Coarse spatial resolution scatterometers (both the ERS-1 Scatterometer and NSCAT) will detect these transformations as a major change in backscatter at the time of thaw, and they will be more sensitive to the earlier stages of this transition than to the final thawing at depth. The shorter the radar wavelength, the less it will penetrate into the scattering surface/volume (vegetation, snow, and soil), and the more sensitive it will be to the initial stages of thaw. The relative contributions of vegetation, snowpack and soil to the backscatter will depend both on the radar

wavelength and on the vegetation canopy density and degree of disturbance (unvegetated land) across the landscape.

4.3. Spring Leaf Area Development at SOA

The NSCAT backscatter signal at the SOA site rises steadily during June 1997, while the SOBS and NOBS backscatter signals do not (Fig. 2). This rise in backscatter was coincident with the development of leaf area in the SOA canopy. We can compare 1994 leaf area index (LAI) development [*Blanken et al.*, 1997] with 1997 NSCAT backscatter for May and June (Fig. 6a). Note that spring came somewhat earlier in 1994 than in 1997, as shown in the accumulating positive degree days observed at Nipawin, Sask. for those years (Fig. 6b). The radar signal will be most sensitive to changes in scatterers whose sizes are greater than or on the order of the radar wavelength (2.14 cm for NSCAT). Thus the size and number of leaves as well as their water content will affect backscatter. It is likely that the NSCAT backscatter was rising for this site because of the growing leaf biomass and total water content of the canopy. Unfortunately, the NSCAT data record ended at the end of June, as leaf area development was nearing completion, so a further test of this will require a longer data set, which should become available with the launch of a follow-on instrument, QuikScat, in the fall of 1998.

4.4. Difference Between Northern and Southern Sites

The predominant difference between the NSCAT backscatter signal at the northern site and the two southern sites was the stronger seasonality of the signal in the north (Fig. 2). This difference between the northern and southern sites could be due to differences in the quantity or quality of the snowpack, and/or to difference in the vegetation canopy. Measured snow depths were similar at both the northern and southern weather stations (see Fig. 3), as were snowpack densities in earlier years [B. Goodison et al., unpublished BOREAS data]. The southern region averaged about 1°C warmer than the northern region during the period of snow cover, and had more periods of near 0°C temperatures than the north, and so might have a different character to its snowpack. However, it was still quite cold at these southern sites (mean Jan. 1997 temperature was -21.7°C) and certainly frozen for most of the winter.

Based on optical remote sensing landcover classifications [*Steyaert et al.*, 1997], the northern BOREAS study area had more fire scars and regenerating vegetation, more rock outcrops and bare ground, generally lower canopy density for the dominant land cover class (wet conifer), and less mixed canopy forests with >50% deciduous vegetation than the southern BOREAS study area. *Chen et al.*, [1997] report leaf area index values for 'disturbed' black spruce sites near NOBS and SOBS at 0.33-1.31, while mature black spruce stand LAI values generally range from 1.5 - 3.0. *Ranson et al.* [1997] reported for jack pine stands in the BOREAS southern study area that trees in regenerating sites (5-10 years since disturbance) had heights of 1-3 m, while mature jack pine forests (70-90 years since disturbance) had tree heights of 13-18 m. Analysis with the Shuttle Imaging Radar (SIR-C) showed a ten-fold increase in above ground biomass between regenerating and mature stands [*Ranson et al.*, 1997]. With more disturbed area and a generally lower canopy density in the north, the ground snow cover would have more influence on the NSCAT backscatter. However, the southern study area had more open water (and larger water bodies) and more agricultural land (generally bare ground in winter). The snowpack in these larger open regions might be different from forest snowpacks, due to greater exposure to wind and direct sunlight. Within the 50 x 50 km cells at the three tower sites selected for this study, however, the landcover differences between south and north (see Table 1) are not as great as the general differences between north and south reported by *Steyaert et al.* [1997]. A further analysis of north-south gradients in the NSCAT signal across a broader region of the boreal ecozone is needed to evaluate this.

4.5. Ecosystem Growing Season Boundaries

The pattern of net ecosystem productivity in the boreal zone is one of a rapid onset of carbon uptake (immediately after snowmelt and soil thaw in evergreen systems, and upon leafout in deciduous systems), highest rates of uptake during the early summer (when light levels are high, water is generally abundant, and soils are still cool), declining uptake in late summer, significant loss (respiration during late autumn and early winter until the soils cool and freeze, and low rates of loss during the bulk of the winter [e.g., *Goulden et al.*, 1997; *Kimball et al.*, 1997; *Black et al.*, 1996; *Frolking et al.*, 1996]. NSCAT's strong

spring thaw signal coincided with the end of the ecosystem's steady winter respiration period (Fig. 7). The NSCAT thaw signal occurred at the beginning of snowmelt; net carbon uptake by the forest ecosystem (positive net ecosystem exchange of CO_2 (NEE) in Fig. 7) began when the snow had completed melting about 30 days later (see Fig. 3a). Because liquid water is abundant across the landscape at snowmelt, the high frequency NSCAT signal will not penetrate into the soil and will be unable to monitor its freeze/thaw state. The end of the growing season occurred in late September 1996 in both model simulations, when diurnal minimum air temperatures were consistently below 0°C. The NSCAT backscatter dropped by about 1 dB at this time (Fig. 7), but this was very near the beginning of the record. Shifts in NSCAT backscatter during the winter did not correspond to major shifts in NEE (Fig. 7) as the soils were cold and the ground snow covered all winter long.

4.6. Conclusions

NSCAT operated for only about 9.5 months, which was not long enough to thoroughly evaluate its potential as an earth system monitoring instrument. A follow-on instrument, QuikScat, with similar characteristics to NSCAT, is scheduled for launch in Nov. 1998. As these data become available, a more complete analysis of the annual cycle and of interannual variability in this cycle will be possible. The NSCAT analysis reported here indicates that K_u-band active microwave scatterometers can bound the growing season in the boreal zone by signaling the arrival of the snowpack and the onset of snowmelt and surface thaw. A direct correlative analysis with vegetation temperature was not possible as in situ measurements were not available during the NSCAT lifetime. However, the arrival and departure of snow is roughly coincident with ecosystem freezing and thawing, though soil freezing can lag snowfall if snowfall is early and heavy, and lead it otherwise, and soil thawing in spring will generally lag snowmelt, except in regions with deep snow and no extreme cold where the soil may never really freeze.

Further analysis at other sites, and with a longer record from a new instrument will be necessary to fully evaluate the ability of this type of instrument to capture both the spring leafout of deciduous ecosystems, and the onset of frost and snow in the autumn, which (along with shorter daylength) signal the end of the

growing season [e.g., *Larcher*, 1993]. A more complete data set on snow, branch, bole, and leave/needle temperatures, and on canopy and ground snowpack texture would lead to a clearer interpretation of both the variability of NSCAT during the winter and the ecosystem significance of the thaw signal in spring. A better understanding of the difference of the NSCAT signal between the northern and southern sites will also be necessary to develop a robust freeze/thaw detection algorithm that accounts for the complete ensemble of vegetation and snow freeze/thaw effects.

ACKNOWLEDGMENTS

This work was supported by grants from the NASA Terrestrial Ecology Program, the National Science Foundation Division of Polar Programs. Portions of the research described in this paper was carried out by the Jet Propulsion Laboratory, California Institute of Technology, under contract with the National Aeronautics and Space Administration. We thank Rob Braswell, Bill Salas, and Xiangming Xiao for helpful discussions, and two anonymous reviewers for helpful comments and suggestions.

REFERENCES

Black, T.A. G. Den Hartog, H.H. Neumann, P.D. Blanken, P.C. Yang, C. Russell, Z. Nesic, X. Lee, S.G. Chen, R. Staebler, and M.D. Novak, Annual cycles of water vapour and carbon dioxide fluxes in and above a boreal aspen stand, *Global Change Biol.*, *2*, 219-229, 1996.

Blanken, P.D., T.A. Black, P.C. Yang, H.H. Neumann, Z. Nesic, R. Staebler, G. den Hartog, M.D. Novak, and X. Lee, Energy balance and canopy conductance of a boreal aspen forest: partitioning overstory and understory components, *J. Geophys. Res.*, *102*, 28915-28927, 1997.

Boehnke, K. and V. Wismann, Detecting soil thaw in Siberia with ERS scatterometer and SAR, *Proc. 3rd ERS symp. on Space at the Service of our Environment*, European Space Agency SP-414, pp. 35-40, 1997.

Chen, J.M., P.M. Rich, S.T. Gower, J.M. Norman, and S. Plummer, Leaf area index of boreal forests: Theory, techniques, and measurements. *J. Geophys. Res.*, *102*, 29429-29444, 1997.

Colbeck, S.C., An overview of seasonal snow metamorphism. *Rev. Geophys. Space Phys.*, *20*, 45-61, 1982.

Dunbar, R.S., NASA Scatterometer High-Resolution Merged Geophysical Data Product User's Guide, version 1.0, NASA Jet Propulsion Lab. Report, 1996.

Elachi, C., *Introduction to the Physics and Techniques of Remote Sensing*, John Wiley & Sons, New York, 413 pp, 1987.

Elliott-Fisk, D.L. (1988)The boreal forest, in: M.G. Barbour and D.W. Billings (eds.) *North American Terrestrial Vegetation*, Cambridge Univ. Press, Cambridge UK, pp. 33-62, 1988.

Frolking, S, M.L. Goulden, S.C. Wofsy, S.-M. Fan, D.J. Sutton, J.W. Munger, A.M. Bazzaz, B.C. Daube, P.M. Crill, J.D. Aber, L.E. Band, X. Wang, K. Savage, T. Moore, and R.C. Harriss, Modelling temporal variability in the carbon balance of a spruce/moss boreal forest, *Global Change Biol.*, *2*, 343-366, 1996.

Frolking, S., Sensitivity of spruce/moss boreal forest carbon balance to seasonal anomalies in weather, *J. Geophys. Res.*, *102*, 29,053-29,064, 1997.

Goulden M.L., J.W. Munger, S.-M. Fan, B.C. Daube and S.C. Wofsy, CO_2 exchange by a deciduous forest: Response to interannual climate variability, *Science*, *271*, 1576-1578, 1996.

Goulden M.L., B.C. Daube, S.-M. Fan, D.J. Sutton, A. Bazzaz, J.W. Munger, and S.C. Wofsy, Physiological responses of a black spruce forest to weather, *J. Geophys. Res., 102*, 28,987-28,996, 1997.

Hall, D.K., M. Sturm, C.S. Benson, A.T.C. Chang, J.L. Foster, H. Garbeil, and E. Chacho, Passive microwave remote sensing and *in situ* measurements of arctic and subarctic snow covers in Alaska, *Remote Sens. Environ., 38*, 161-172, 1991.

Hall, F.G., D.E. Knapp, and K.F. Huemmrich, Physically based classification and satellite mapping of biophysical characteristics in the southern boreal forest. *J. Geophys. Res., 102*, 29567-29580, 1997.

Jarvis P.G., J.M. Massheder, S.E. Hale, J.B. Moncrieff, M. Rayment, and S.L. Scott, Seasonal variation of carbon dioxide, water vapor, and energy exchanges of a boreal black spruce forest. . *J. Geophys. Res., 102*, 28953-28966, 1997.

Keeling, R.F., S.C. Piper and M. Heimann, Global and hemispheric CO_2 sinks deduced from changes in atmospheric O_2 concentration. *Nature, 381*, 218-221, 1996.

Kennett, R.G., and F. Li, Seasat over-land scatterometer data, Part I: Global overview of the Ku-band backscatter coefficients, *IEEE Trans. Geosci. Remote Sens., 25*, 592-605, 1989.

Kimball, J.S., P.E. Thornton, M.A. White, and S.W. Running, Simulating forest productivity and surface-atmosphere carbon exchange in the BOREAS study region, *Tree Physiol.,* 17, 589-599, 1997.

Kraszewski, A (ed.), *Electromagnetic Wave Interaction with Water-Containing Materials*, IEEE Press, Piscataway NJ, 484 pp, 1996.

Kunzi, K.F., S. Patil, and H. Rott, Snow-cover parameters retrieved from Nimbus-7 scanning multichannel microwave radiometer (SMMR) data, *IEEE Trans. Geosci. Remote Sens., 20*, 452-467, 1982.

Larsen, J.A., *The Boreal Ecosystem*, Academic Press, NY, 500 pp, 1980.

Larcher, W., *Physiological Plant Ecology*, Springer-Verlag, Berlin, 506 pp, 1993.

Myneni RB, Keeling CD, Tucker CJ, Asrar G, Nemani RR, Increased plant growth in the northern high latitudes from 1981-1991. *Nature, 386*, 698-702, 1997.

Naderi, F.M., M.H. Freilich, and D.G. Long, Spaceborne Radar Measurement of Wind Velocity over the Ocean--An Overview of the NSCAT Scatterometer System. *Proceedings of the IEEE, 79*, 6, 1991.

Ranson, K.J., G. Sun, R.H. Land, N.S. Chauhan, R.J. Cacciola, and O. Kilic, Mapping of boreal forest biomass from spaceborne synthetic aperture radar. *J. Geophys. Res.*, *102*, 29599-29610, 1997.

Rignot E., and J.B. Way, Monitoring freeze-thaw cycles along north-south Alaskan transects using ERS-1 SAR, *Remote Sens. Environ.*, 49, 131-137, 1994.

Rignot E., J.B. Way, K. McDonald, L. Viereck, C. Williams, P. Adams, C. Payne, W. Wood, and J. Shi, Monitoring of environmental conditions in taiga forests using ERS-1 SAR, *Remote Sens. Environ., 49*, 145-154, 1994.

Saatchi S.S. and E. Rignot. 1997. Classification of boreal forest cover types using SAR images, *Remote Sensing of Environment, 60*:270-281.1997.

Sellers, P.J., F.G. Hall, R.D. Kelly, and 18 others. BOREAS in 1997: Experiment overview, scientific results, and future directions, *J. Geophys. Res. 102*, 28731-28770, 1997.

Shi, J., R.E. Davis, and J. Dozier, Stereological determination of dry-snow parameters for discrete-scatterer microwave modeling, *Annals Glaciol.*, 17, 295-299, 1993.

Steyaert L.T., F.G. Hall, T.R. Loveland, Land cover mapping, fire regeneration, and scaling studies in the Canadian boreal forest with 1 km AVHRR and Landsat TM data. *J. Geophys. Res. 102*, 29581-29598, 1997.

Tsai, W., J. Graf, C. Winn, J. Huddleston, S. Dunbar, M. Freilich, F. Wentz, D. Long and L. Jones, Post-launch sensor verification and calibration of the NASA Scatterometer, Submitted to *IEEE Trans. Geosci. Remote Sens.*, 1998.

Ulaby, F.T., R.K. Moore, and A.K. Fung, *Microwave Remote Sensing--Active and Passive*, vol. II, Artec House, Norwood, Mass., pp. 457-1064, 1982.

Wankiewicz, A. Multi-temporal microwave satellite observations of snowpacks. *Annals Glaciol., 17*, 155-160, 1993.

Way, J.B., E. Rignot, R. Oren, R. Kwok, K. McDonald, M.C. Dobson, G. Bonan, L. Viereck, and J.E. Roth Evaluating the type and state of Alaskan taiga forests with imaging radar to use in ecosystem flux models, *IEEE Trans. Geosci. Remote Sens., 32*, 353-370, 1994.

Way, J.B., R. Zimmermann, E. Rignot, K. McDonald, R. Oren, Winter and spring thaw as observed with imaging radar at BOREAS. *J. Geophys. Res. 102*, 29673-29684, 1997.

Wegmuller, U., The effect of freezing and thawing on the microwave signatures of bare soil. *Remote Sens. Environ., 33*, 123-135, 1990.

Table 1. Proportional cover within 50 x 50 km window centered over tower-flux sites

	Landsat TM[1]			AVHRR[1]		
CLASS	SOA[2]	SOBS	NOBS	SOA	SOBS	NOBS
Dry conifer	0.01	0.01	0.02	<0.01	0.02	0.09
Wet conifer	0.20	0.37	0.08	0.02	0.60	0.50
Mixed deciduous-conifer	0.23	0.13	0.06	0.61	0.25	0.30
Deciduous	0.29	0.08	0.20	--[3]	--	--
Regenerating conifer	0.05	0.16	0.20	--	--	--
Regenerating deciduous	0.11	0.05	0.16	--	--	--
Disturbed[4]	0.01	0.02	0.02	0.35	0.07	0.08
Fen	0.03	0.10	0.19	<0.01	<0.01	<0.01
Fire blackened	<0.01	<0.01	<0.01	--	--	--
Grass	0.01	<0.01	<0.01	--	--	--
Open water	0.08	0.09	0.06	0.01	0.07	0.03

1. [*Steyaert et al.*, 1997]

2. TM data only cover 57% of this window; there are no data for areas in the S-SW; proportions are relative to the area of actual data.

3. not a Landsat TM class in this analysis.

4. This disturbed class included agricultural land in the AVHRR analysis.

Table 2. Statistics of NSCAT backscatter (smoothed first differences).

site	n	mean (dB)	S[1]	# days outside 2S	June mean (dB)	Feb. mean (dB)
NOBS PM	277	0.003	0.297	16	-11.283	-8.377
NOBS AM	276	0.010	0.223	14	-10.727	-8.343
SOBS PM	278	-0.004	0.308	16	-11.015	-9.908
SOBS AM	275	0.000	0.262	15	-10.691	-9.978
SOA PM	279	-0.001	0.316	16	-10.108	-10.211
SOA AM	275	0.006	0.332	11	-9.855	-10.450

1. S = standard deviation.

Table 3. Northern Sites Anomalous Backscatter[1] and Local Weather

yearday	NOBS PM	NOBS AM	Weather at Thompson, Manitoba
27-Sep-96	**++**[2]		T_{min}<0 (not first of year)
28-Sep-96	**--**		light snow
14-Oct-96	**--**		new snow (T~0°C)
15-Oct-96	**++**		new snow (T~0°C)
16-Oct-96	**++**		rain on snow (T~0°C)
31-Oct-96	+		new snow
2-Nov-96		**++**	???
3-Nov-96		**++**	maybe new snow
4-Nov-96	+	**++**	maybe new snow
7-Nov-96		-	new snow
25-Nov-96		-	new snow, but shallower; extreme cold
28-Mar-97		-	new snow
31-Mar-97		+	snowmelt
6-Apr-97	**++**	**++**	new snow
7-Apr-97	**++**	**++**	new snow
14-Apr-97	-	-	snowmelt
17-Apr-97	**--**	**--**	snowmelt & T_{max}>0, T_{min} <0
18-Apr-97	**--**	**--**	snowmelt & T_{max} >0, T_{min} <0
20-Apr-97	**--**	-	snowmelt & T_{max} >0, T_{min} <0
21-Apr-97	**--**		snowmelt & T_{max} >0, T_{min} <0
22-Apr-97	**--**	-	snowmelt & T_{max} >0, T_{min} <0
27-Apr-97	+		snowmelt & T_{max} >0, T_{min} <0

1. '+' for positive anomaly, '-' for negative anomaly; blank or not listed if not anomalous (see Fig. 3).
2. Consecutive days with anomalies have double symbols and are in boldface.

Table 4. Southern Sites Anomalous backscatter[1] and Local Weather

yearday	SOBS PM	SOBS AM	SOA PM	SOA AM	Weather at Nipawin, Sask.
23-Sep-96		+			???
26-Sep-96	+				???
28-Sep-96	-	-			???
15-Oct-96	+				T_{min} <0, but not first of year
16-Oct-96			-		???
21-Oct-96	-				T_{min}<0
24-Oct-96		-			T_{max} <0 (first of year)
25-Oct-96			-		new snow
2-Nov-96		-			new snow (also day 304-5)
1-Dec-96			-		???
26-Dec-96			+		some snowmelt
13-Jan-97			+		some snowmelt
19-Jan-97	-	-	-		extreme cold (6th day of cold)
24-Jan-97	+	+	+	+	???
21-Mar-97				--[2]	new snow
22-Mar-97				--	new snow
29-Mar-97	+	++	+	++	??
30-Mar-97		++		++	??
31-Mar-97	+			++	new snow
1-Apr-97		++			new snow
2-Apr-97		--			???
3-Apr-97	-				new snow
5-Apr-97		+			T_{max} > 0 (not first of year)
6-Apr-97	++		++		T_{max} > 0 & new snow
7-Apr-97	++	+	++	+	T_{max} > 0
9-Apr-97	+		++		snowmelt
10-Apr-97			++	+	snowmelt
12-Apr-97	--	--	--		prob. rain
13-Apr-97	--	--	--	--	snowmelt
14-Apr-97	--	--	-	--	snowmelt
15-Apr-97				--	snowmelt
20-Apr-97	-		-		new snow

1. '+' for positive anomaly, '-' for negative anomaly; blank or not listed if not anomalous (see Fig. 3).
2. Consecutive days with anomalies have double symbols and are in boldface.

FIGURE CAPTIONS

1. Observed [*Goulden et al.,* 1997] and simulated [*Frolking et al.*, 1996] 5 cm soil temperature for the BOREAS NOBS stand (a) with a relatively open canopy and *Sphagnum* moss ground cover, and (b) with a relatively closed canopy and feathermoss ground cover. In both cases the surface organic horizon was greater than 15 cm thick, so the data and simulations represent conditions within the organic layer under the live moss.

2. NASA Scatterometer (NSCAT) microwave backscatter for morning (AM) and afternoon (PM) overflights of the (a) NOBS, (b) SOBS, and (c) SOA BOREAS tower sites. NSCAT was operational from 15 Sept. 1996 through 28 June 1997.

3. NSCAT backscatter (heavy black line), observed diurnal air temperature range (gray bars) and snow depth (dashed line), and simulated 5 cm soil temperature (thin black line) for the (a) NOBS, (b) SOBS, and (c) SOA BOREAS tower sites for 15 Sept. 1996 through 28 June 1997. The diurnal air temperature range is plotted as a gray vertical bar extending each day from the minimum to the maximum air temperature. Soil temperature simulations were done with the model of *Frolking et al.* [1996].

4. First differences of the 5-day smoothed AM & PM NSCAT backscatter for the (a) NOBS, (b) SOBS, and (c) SOA BOREAS tower sites for 15 Sept. 1996 through 28 June 1997 (see text for details of calculations). The shaded regions in each panel represent two standard deviations around the mean first differences for each site (see Table 3). 'Anomalous' first differences, greater than two standard deviations from the mean occur in the fall and spring at all three sites, and during the winter at SOBS and SOA. See Table 4 for an evaluation of the anomalous dates.

5. Five-day smoothed NSCAT backscatter for the NOBS, SOBS, and SOA BOREAS tower sites for 15 Sept. 1996 through 28 June 1997. This smoothing combined AM PM overflight data. The horizontal

lines represent the mean of February (frozen) and June (thawed) mean NSCAT backscatter for each site, and thus a proposed freeze/thaw threshold [*Boehnke & Wismann*, 1997].

6. (a) Five-day smoothed NSCAT backscatter for the SOA BOREAS tower site for 15 May through 28 June 1997 (hatched squares) and observed total leaf area index development (solid circles) at the SOA BOREAS tower site in 1994 [*Blanken et al.*, 1997]. The rise in NSCAT backscatter over this interval appears to be coincident with deciduous vegetation leaf development. (b) Accumulating positive degree days at the SOA BOREAS tower site in 1994 (solid line) and 1997 (dashed line); note that warming in 1994 occurred earlier than in 1997, so leaf development in 1994 probably also occurred earlier than in 1997.

7. Five-day smoothed NSCAT backscatter for the NOBS BOREAS tower site, and five-day smoothed net ecosystem exchange of carbon dioxide (NEE) for this site as simulated by the Boreal Forest Carbon Model (BFCM [*Frolking et al.*, 1996]) and BIOME-BGC [*Kimball et al.*, 1997]. The sign convention used is for positive NEE to mean net ecosystem uptake of CO_2 from the atmosphere.

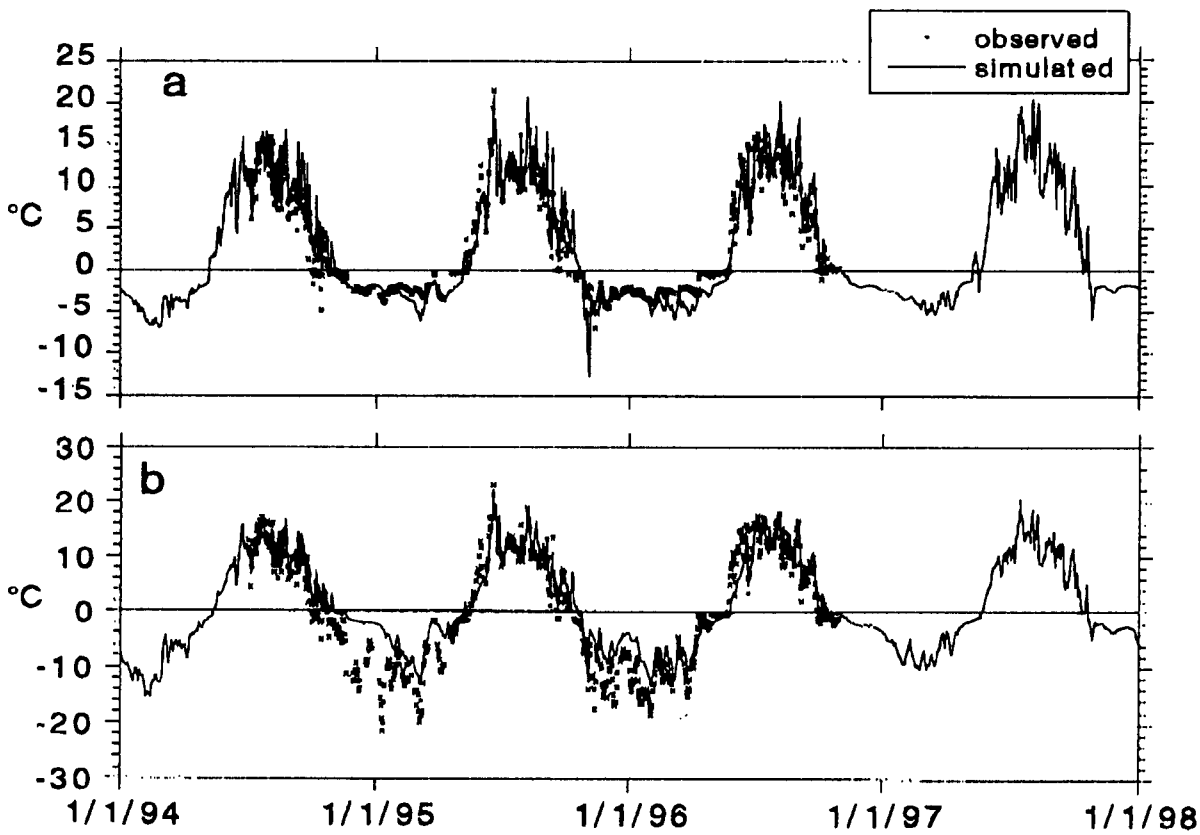
observed
simulated
a
b
°C
°C
25
20
15
10
5
0
-5
-10
-15
30
20
10
0
-10
-20
-30
1/1/94
1/1/95
1/1/96
1/1/97
1/1/98

Fig 1

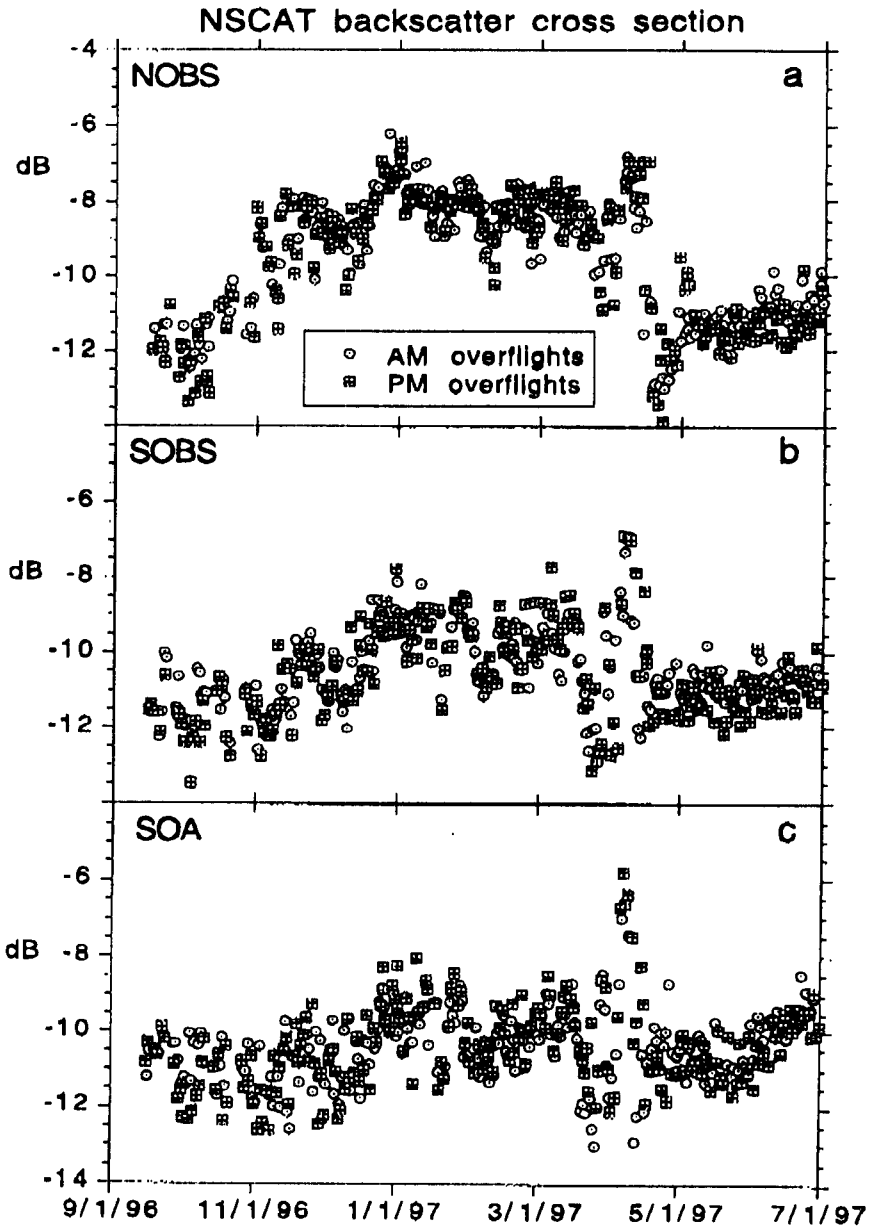
NSCAT backscatter cross section
NOBS
a
SOBS
b
SOA
c
dB
-4
-6
-8
-10
-12
-14
AM overflights
PM overflights
9/1/96
11/1/96
1/1/97
3/1/97
5/1/97
7/1/97

Fig. 2.

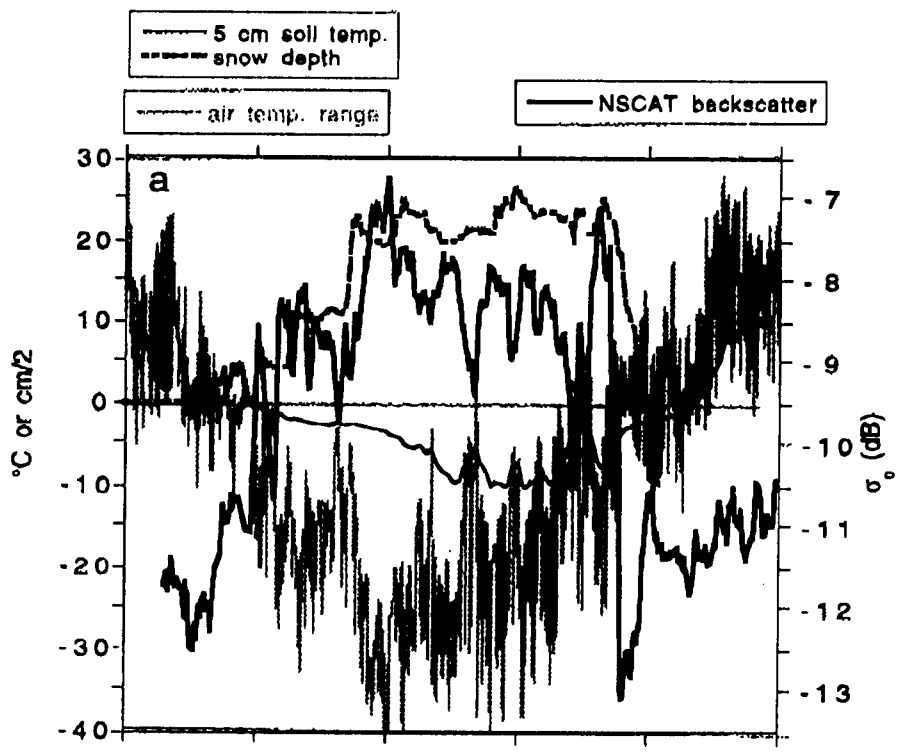
5 cm soil temp.
snow depth
air temp. range
NSCAT backscatter
a
30
20
10
0
-10
-20
-30
-40
°C or cm/2
-7
-8
-9
-10
-11
-12
-13
σ° (dB)

Fig 3a

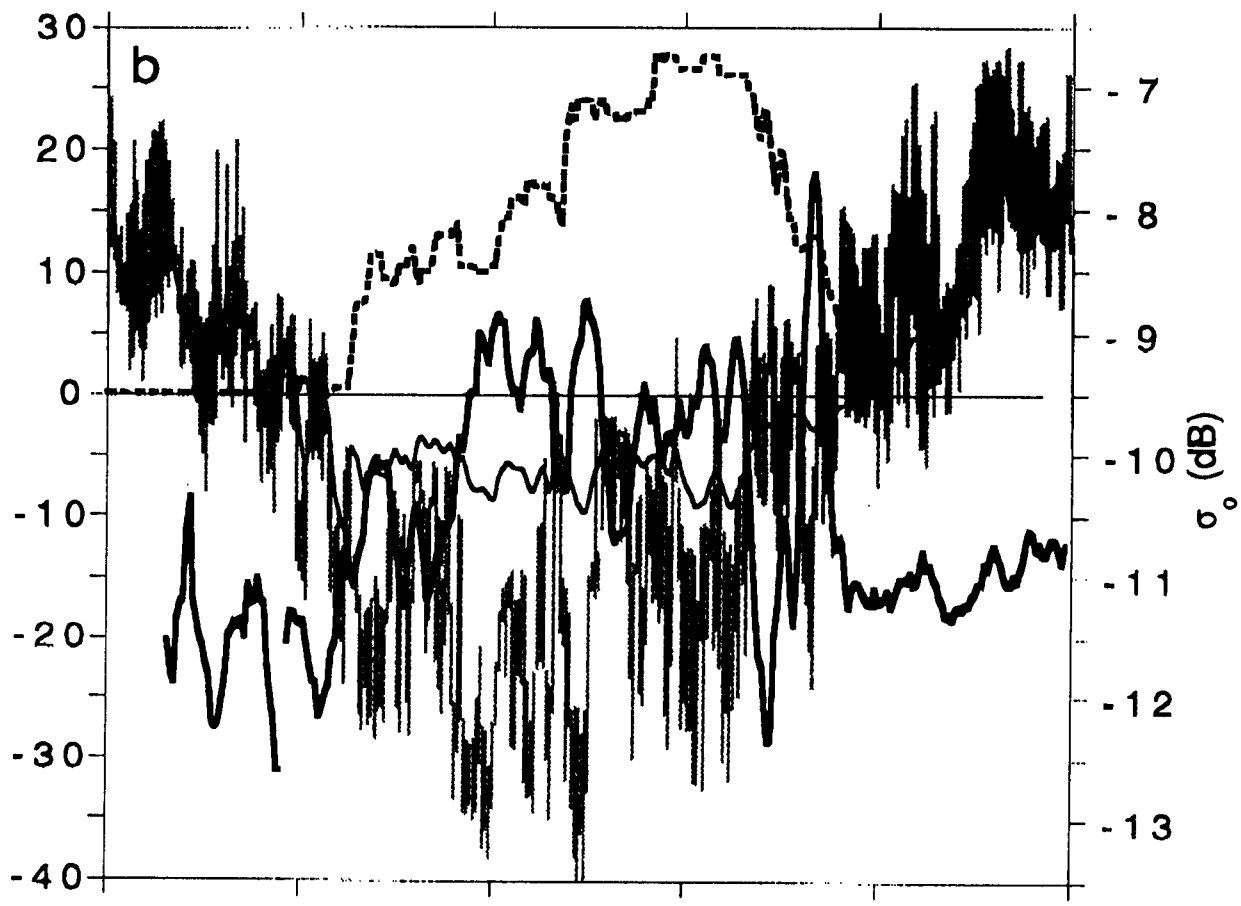

Fig 3b

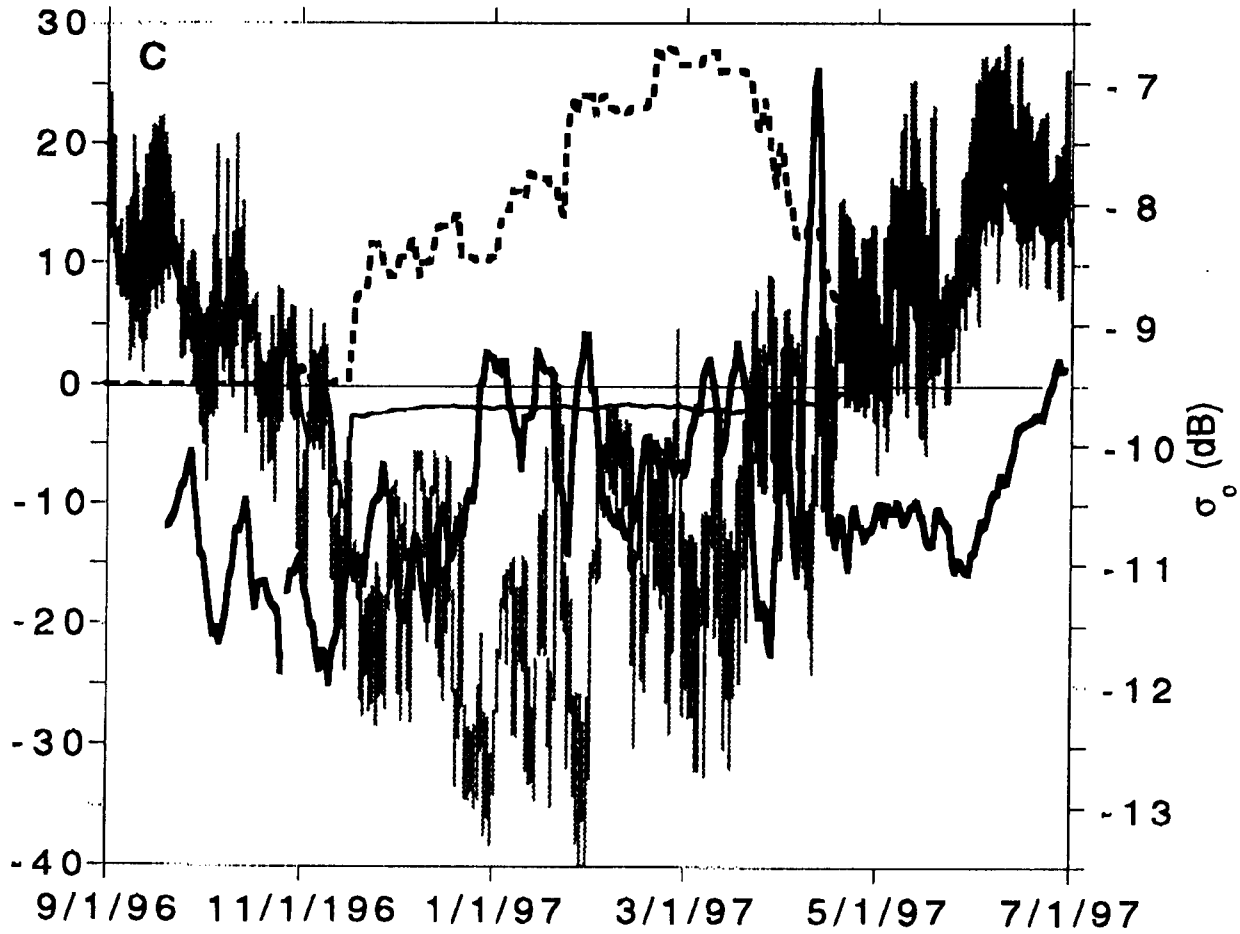
C
30
20
10
0
-10
-20
-30
-40
-7
-8
-9
-10
-11
-12
-13
σ° (dB)
9/1/96
11/1/196
1/1/97
3/1/97
5/1/97
7/1/97

Fig 3a

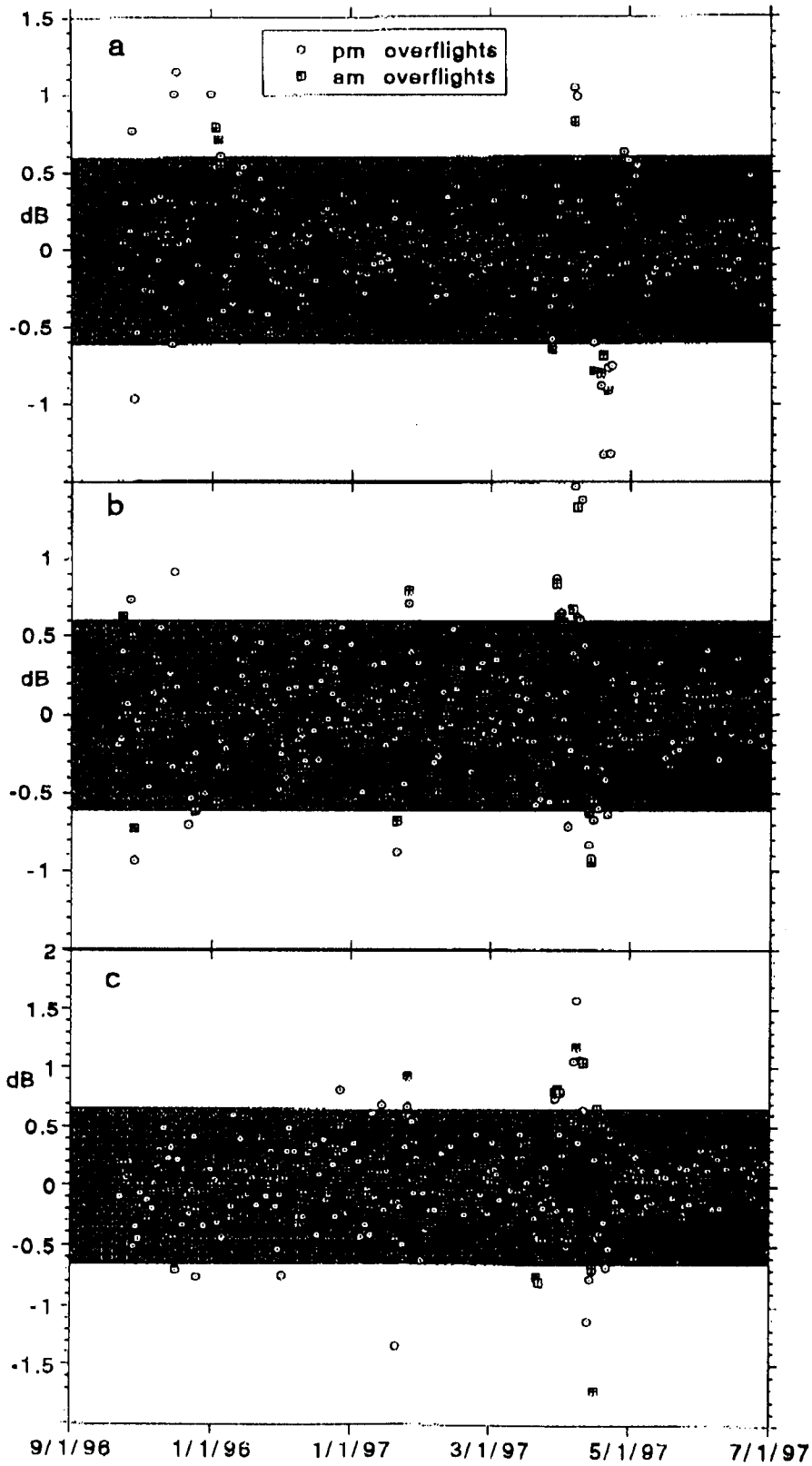
a
pm overflights
am overflights
b
c
dB
1.5
1
0.5
0
-0.5
-1
2
-1.5
9/1/96
1/1/96
1/1/97
3/1/97
5/1/97
7/1/97

fig 4

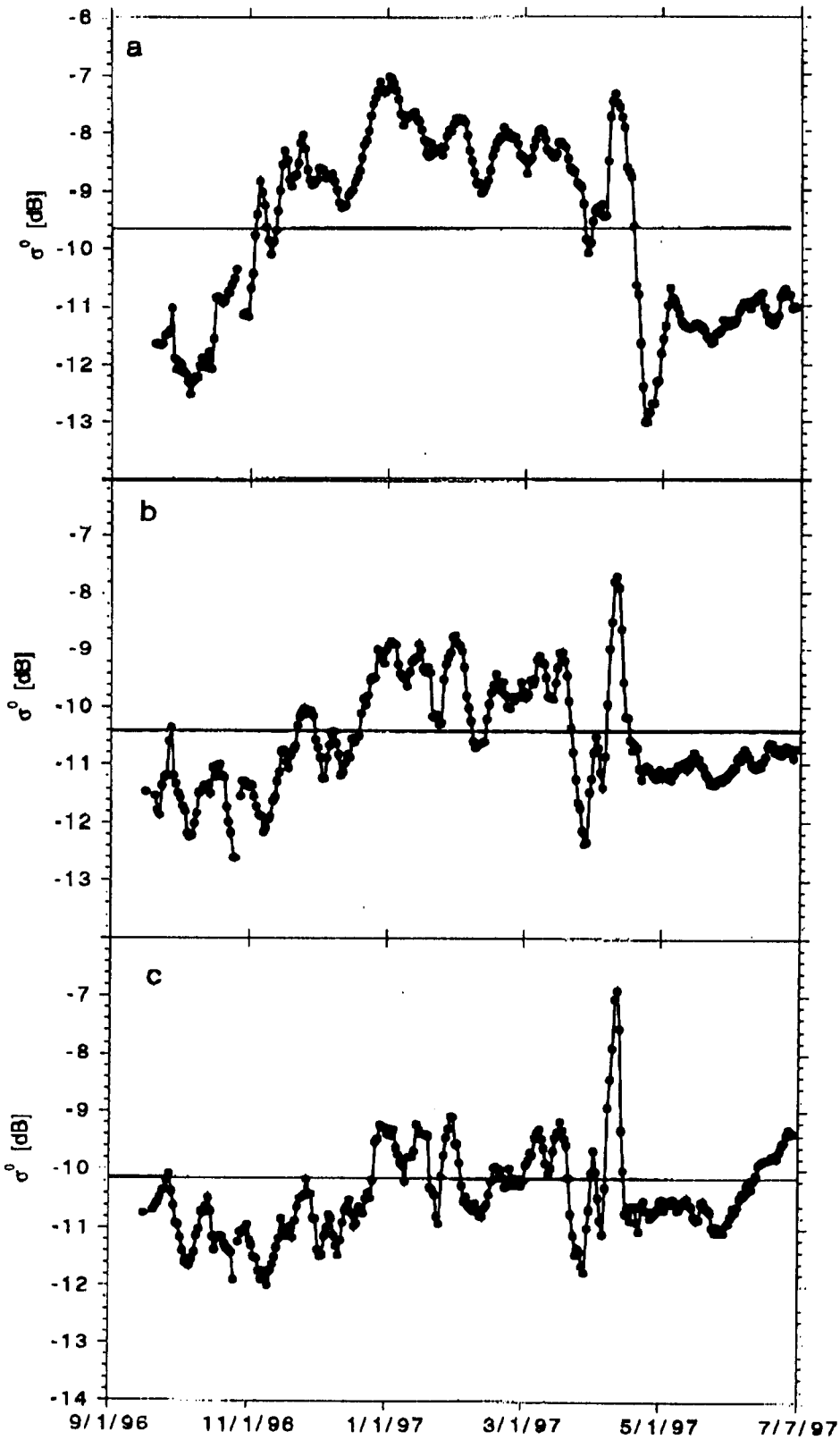

fig 5

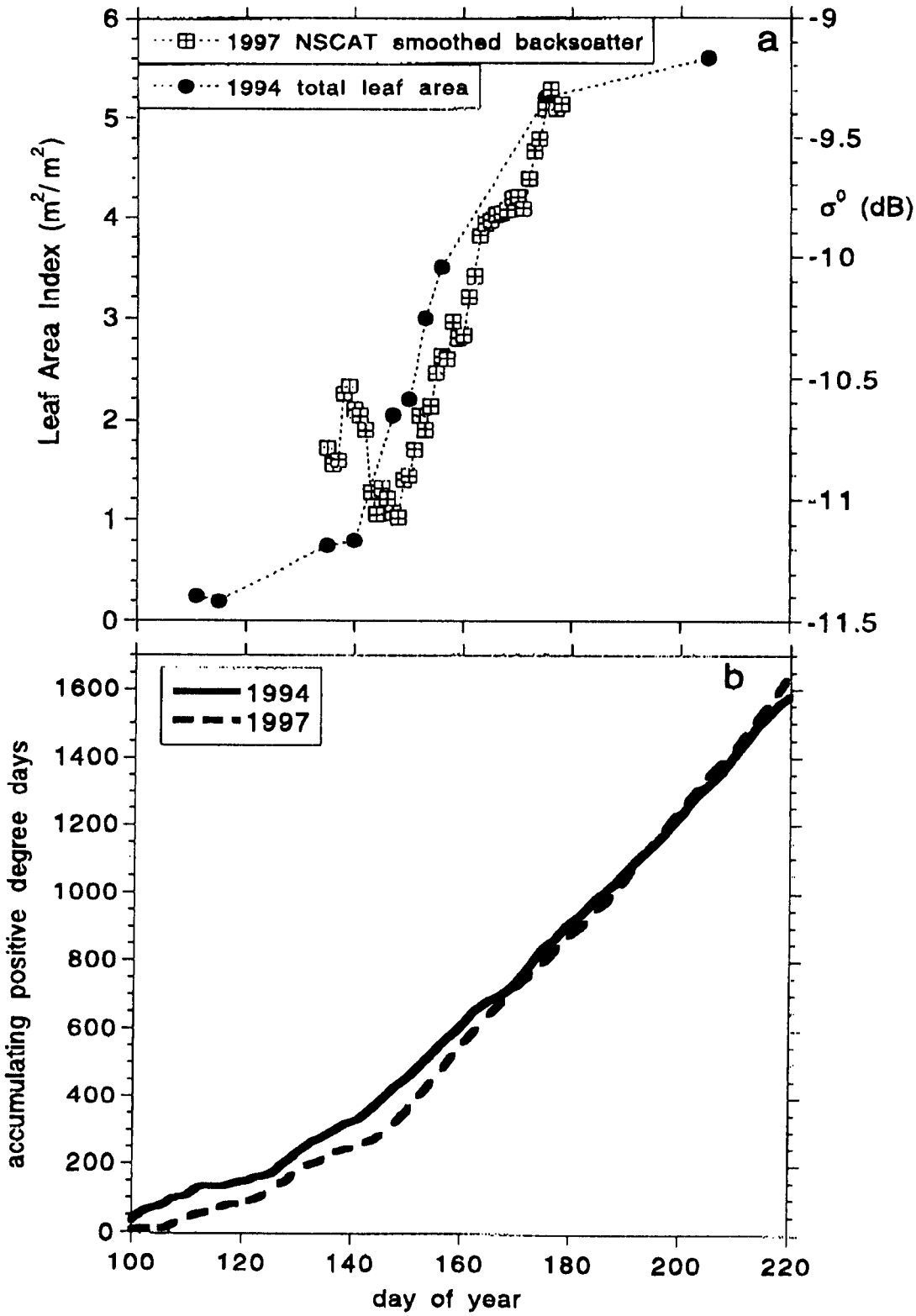
1997 NSCAT smoothed backscatter
1994 total leaf area
a
Leaf Area Index (m²/m²)
σ° (dB)
6
5
4
3
2
1
0
-9
-9.5
-10
-10.5
-11
-11.5
b
1994
1997
accumulating positive degree days
1600
1400
1200
1000
800
600
400
200
0
100
120
140
160
180
200
220
day of year

fig 6

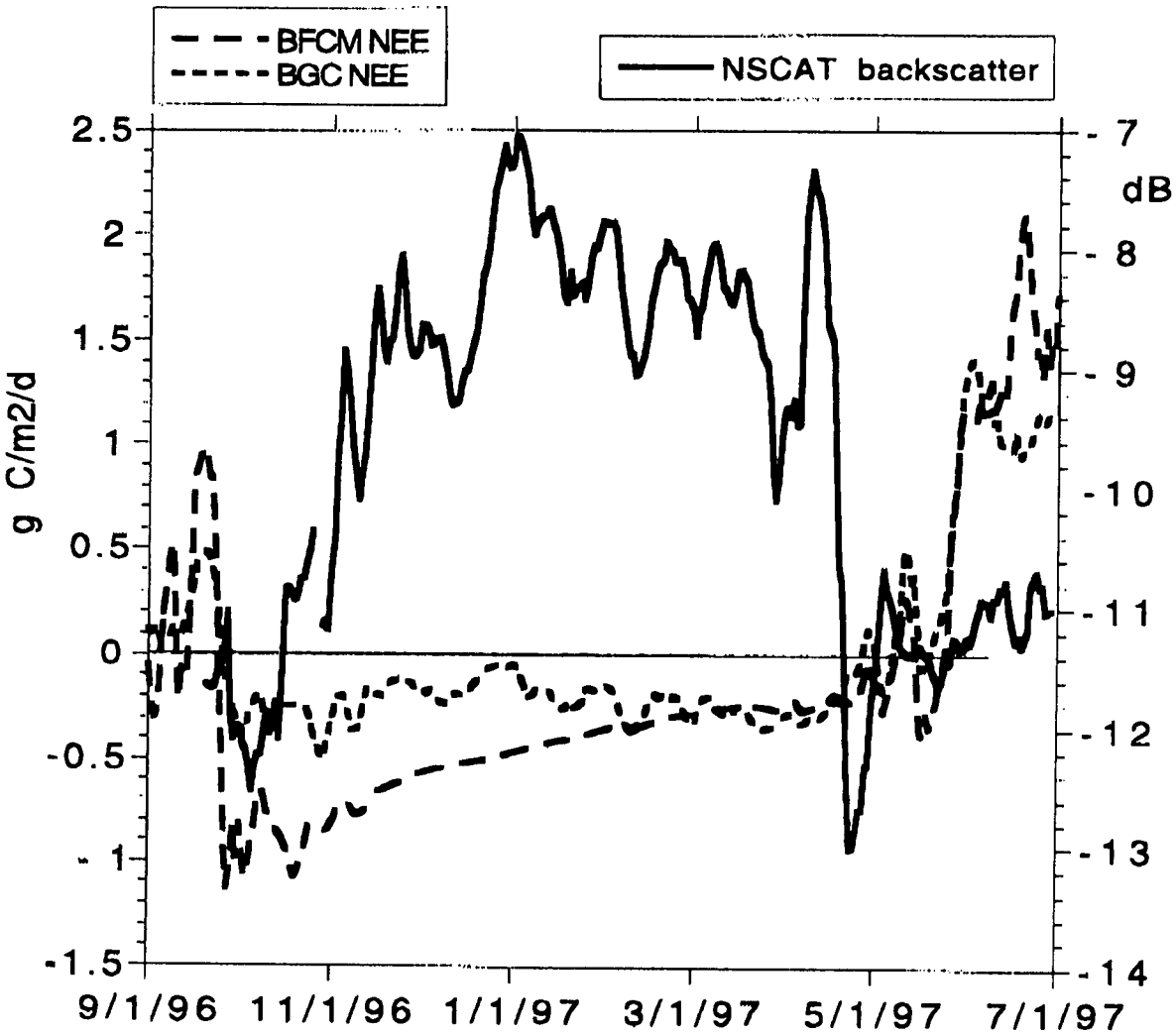
BFCM NEE
BGC NEE
NSCAT backscatter
g C/m2/d
dB
2.5
2
1.5
1
0.5
0
-0.5
-1
-1.5
-7
-8
-9
-10
-11
-12
-13
-14
9/1/96
11/1/96
1/1/97
3/1/97
5/1/97
7/1/97

fig 7